Paper No. 83. Bulletin of the Indian Society of Earthquake Technology, Vol. VII, No. 1, pp. 25-40, March 1970

TRANSIENT RESPONSE OF DAM-LIKE STRUCTURE SUBJECTED TO EARTHQUAKE

S. Basu* and A. V. Setlur***

INTRODUCTION

The earthquake at Koyna on December 11, 1967, where a concrete gravity dam of major importance is situated, has revived the interest in the deeper study of transient response of dam structures subjected to earthquake motions.

A study through the literature indicates that there are available, in general, three techniques for the theoretical analysis of transient stresses in elastic bodies caused by such dynamic loadings. These methods are :

(i) The method of mode superposition

(ii) The Laplace transform technique

(iii) The method of characteristic and numerical integrations.

The method of mode superposition which is by far the most popular technique, utilizes the normal mode of vibration of the body along with the response spectra for the earthquake record to obtain the maximum response developed for any given natural frequency of vibration. The drawback of the procedure is that it tends to round-off the peaks of the response characteristics. The Laplace transform has its inherent inversion difficulties and frequently numerical methods of integration have to be developed to evaluate the integrals of the transform.

The method of characteristics is ideally suited for transient response studies. The advantages of this approach are :

(a) the problem can be formulated a continuous one i. e. no discritization of the physical model is needed.

(b) It gives a simple description of the wavefronts.

(c) Well known technique of numerical integration can be effectively used.

The method of characteristics was used by Leonard and Budiansk[8] to solve for the transient response of a Timoshenko Beam subjected to several types of dynamic loading. Later, the method was further utilised to find transient response of beam, plate, slab and shell problems[3,4,7,9,10]. However, most of the problems solved were either two characteristics problems or for a system having semi-infinite length of structure so that reflection from the support did not arise.

In this paper a method is proposed to evaluate transient response of dam-like structure of finite span using method of characteristics.

---

* Post-graduate Student, Department of Civil Engineering, Indian Institute of Technology, Kanpur

** Assistant Professor, Department of of Civil Engineering, Indian Institute of Technology, Kanpur

BASIC EQUATIONS, INITIAL AND BOUNDARY CONDITIONS

Concrete gravity dams are generally cast in monoliths. The joint between two subsequent monoliths are packed with water-proof materials to prevent water leakage. For reduction of thermal stresses, it is customary to avoid any interconnection of two adjacent monoliths (Fig. 1). After the earthquake on 11th December, 1967 independent deformation of adjacent monoliths of the Koyna-concrete dam has been clearly noticed. Also these monoliths are generally thin compared to the height and width of the cross-section and hence may be assumed in plane stress. Furthermore, it is assumed in the present analysis that the monolith acts as cantilever beams (Fig. 2). Since the width of the dam section is comparable to the height of the dam, shear deformation and rotary in ertia are included in this analysis.

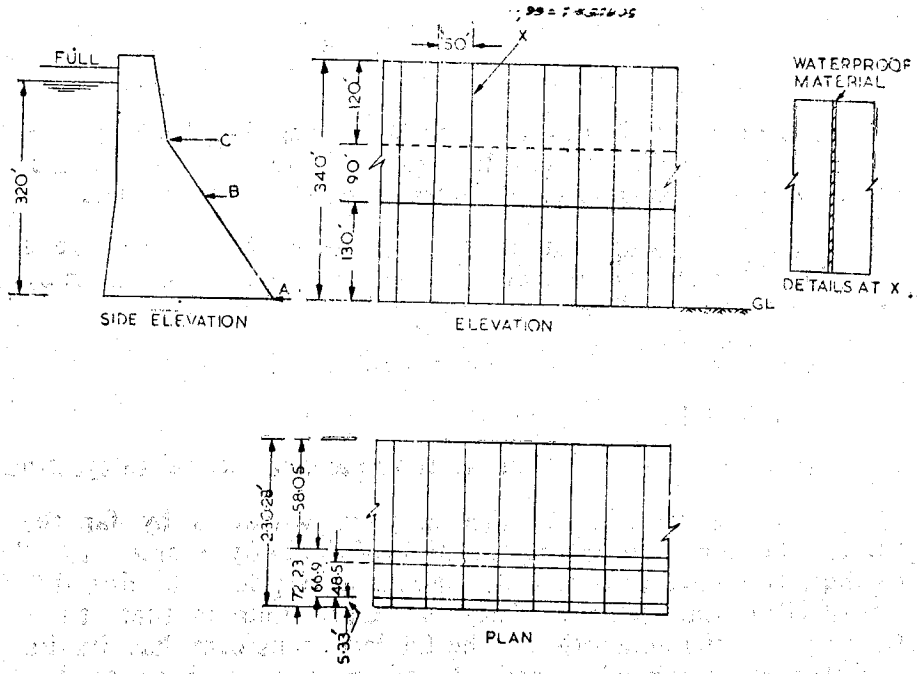

Fig. 1. Structural Details of Dam

The following assumptions are made in the theoretical development :

(i) The material of the dam (concrete) is linearly elastic, isotropic and homogeneous.

(ii) Damping is of the viscous type. The damping coefficient, $\bar{C}$, is assumed to be a percentage of the critical damping C for the fundamental mode, i.e.,

$$\bar{C} = \mu C \tag{1}$$

In Eq. (1), μ is the damping coefficient and generally ranges between 0.05 and 0.15 and

$$C = 2 \rho A \omega_1 \tag{2}$$

where,

ρ = density of concrete

A = cross-sectional area of monolith at a particular height of dam

ω_1 = fundamental frequency of the system

(iii) Effect of cracking in concrete is neglected.

(iv) The impounding water is incompressible and is subjected to irrotational flow of small amplitude. Zanger's[11] hydrodynamic pressure distribution is assumed. It may be noted that though the virtual mass addition concept does not adequately represent the effect of the impounding water[2], it is used in this analysis for simplicity. The hydrodynamic effect due to deformation of the monolith is neglected in accordance with Zanger's theory[11]. Moreover, this effect is excluded

in this analysis since inclusion of it leads to artificial change in the density of the concrete, which in turn changes the speed of wave propagation in the concrete and thus gives rise to a contradiction of physical situation.

The equation of dynamic equilibrium considering a unit width of the assumed physical model subjected to ground acceleration $\ddot{Z}$ are given as follows :

$$M + E\,I\,\psi' = 0 \qquad (3\,a)$$

$$V - k\,A\,G\,(w' - \psi) = 0 \qquad (3\,b)$$

$$M' + \rho\,J\,\ddot{\psi} - V = 0 \qquad (3\,c)$$

$$V' - \rho A\ddot{w} - \overset{*}{\rho}\,\overset{*}{A}\,\ddot{Z} - \bar{C}\,\ddot{w} = 0 \qquad (4\,d)$$

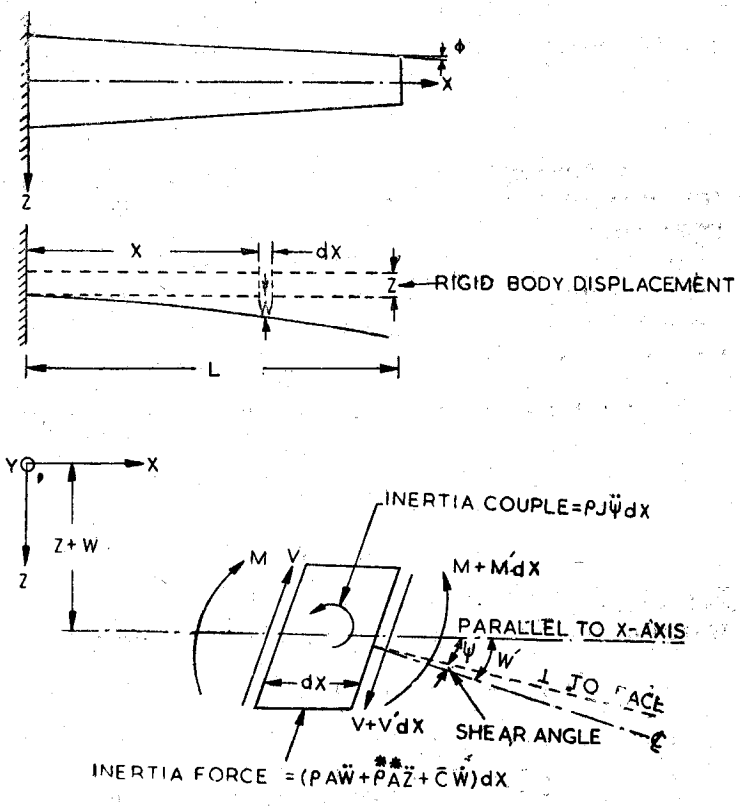

Fig. 2. Force Acting on An Element of Monolith

In Eq. (3) w, ψ, M and V are the transverse deflection relative to the base, bending slope, bending moment and shear force at any cross-section respectively, I, J, k, are the moment of inertia, rotary inertia and form factor respectively. Here a prime denotes partial differentiation with respect to x and a dot that with respect to t. In the foregoing Eq. (3)

$$\overset{*}{\rho}\,\overset{*}{A} = \rho\,A + \rho_w\,A_w \qquad (4)$$

where, $\rho_w\,A_w$ is the virtual mass of water moving along with the dam per foot width of the monolith at a given height, x, from the base of the monolith and given by Zanger's theory as :

$$\rho_w\,A_w = 0.5\,\rho_w\,C_m\,H\left[1 - \frac{x^2}{H^2} + \sqrt{1 - \frac{x^2}{H^2}}\right] \qquad (5)$$

where,

H = height of impounding water

ρ_w = density of impounding water

C_m = pressure coefficient depending on the angle of intersection of the upstream face with vertical.

The initial and boundary conditions of the system of Eqs. (3) may be given as follows :

$$w\,(x, 0) = \dot{w}\,(x, 0) = \psi\,(x, 0) = \dot{\psi}\,(x, 0) = 0 \qquad (6)$$

$$w\,(0, t) = \psi\,(0, t) = M\,(L, t) = V\,(L, t) = 0 \qquad (7)$$

In the Eq. (7), L refers to the total height of the monolith.

The system of Eq. (3), along with initial condition Eq. (6) and boundary conditions Eq. (7), may be solved to obtain response of the monolith subject to earthquake motions.

DERIVATION OF COMPATIBILITY CONDITION

Disturbing forces in the structure are created by the ground acceleration $\ddot{Z}$, which, for an earthquake motion; is a highly irregular function with respect to time Analytic representation of this acceleration–time chart is rather difficult. Thus closed form solution of the governing differential equation is not possible Here a numerical method of solution of the problem is adopted. To facilitate numerical integration, it is advantageous to change the system of Eq. (3) along with initial condition Eq (6) and boundary condition Eq. (7) from a physical plane (x, t) to the characteristic form.

Differentiation of Eqs. (3a and 3b) with respect to t yields :

$$\dot{M} + E\,I\,\dot{\psi}' = 0 \tag{8a}$$

$$\dot{v} - k\,A\,G\,(\dot{w}' - \dot{\psi}) = 0 \tag{8b}$$

Eqs (8a, 8b, 3c and 3d) form a system of four simultaneous partial differential equations which in the non-dimensional form are given by :

$$\dot{\bar{M}} + \bar{I}\,\bar{a}' = 0 \tag{9 a}$$

$$\frac{\dot{\bar{v}}}{\zeta \bar{A}} - \bar{v}' + \frac{k_1}{k_2}\,\bar{a} = 0 \tag{9 b}$$

$$\bar{M}' + \bar{J}\,\dot{\bar{a}} - \bar{V} = 0 \tag{9 c}$$

$$\frac{\bar{V}'}{\bar{A}} - \lambda\,\dot{\bar{v}} - \beta\,\bar{v} - \eta\,\alpha\,f = 0$$

where, $f = \ddot{Z}/g$ (10)

k_1 = propagation velocity of flexural wave $= \sqrt{\dfrac{E\,I_o}{\rho\,J_o}}$

k_2 = propagation velocity of shear wave $= \sqrt{kG/\rho}$

$\bar{a}$ = non-dimensional angular velocity $= \dot{\psi}$

$\bar{v}$ = non-dimensional linear velocity $= \dfrac{k_1}{k_2}\,\dot{w}$

$$\xi = \frac{A_o\,L^2}{J_o}\,(k_2/k_1)^3$$

$$\lambda = \frac{k_2\,A_o\,L^2}{k_1\,J_o}$$

$$\beta = \frac{2\mu\,\omega_1\,\rho\,A_o\,L^3\,k_2}{E\,I_o}$$

$$\alpha = 1.0 + \frac{\rho_w A_w}{\rho A}$$

$$\eta = \frac{\rho g A_0 L^3}{EI_0}$$

In Eq (9) the dot and prime refer to partial differentiation with respect to $\bar{t} = k_1 t/L$ and with respect to $\bar{x} = x/L$ respectively and will be used hence forth except for Eq. (10) where dot refers partial differentiation with respect to t. Also all barred quantities are nondimensional form of unbarred quantities and subscripts zero refers to the cross-section at base. It is also to be noted that parameter α is equal to unity when there is no water in the reservoir basin or when the hydrodynamic effect of water is neglected.

The initial conditions Eq.(6) and boundary conditions Eq.(7) correspondingly changes to

$$\bar{w}(\bar{x},0) = \dot{\bar{v}}(\bar{x},0) = \psi(\bar{x},0) = \bar{a}(\bar{x},0) = 0 \tag{11}$$

$$\bar{w}(0,\bar{t}) = \psi(0,\bar{t}) = \bar{M}(1,\bar{t}) = \bar{V}(1,\bar{t}) = 0 \tag{12}$$

Along a characteristic direction of the system of Eq. (9) discontinuity of the first derivative of dependent variables ($\bar{a}$, $\bar{v}$, $\bar{M}$, $\bar{V}$) along its normal direction, is possible. Given initial data on such a direction the normal derivative of the variables are not uniquely determined by the Eq. (9). However, in the region of $\bar{x}$, $\bar{t}$ plane where the dependent variables are continuous, the following type of relation of each dependent variables must be satisfied :

$$d\bar{M} = \bar{M}' d\bar{x} + \dot{\bar{M}} d\bar{t} \tag{13}$$

The Eq. (9) and type of Eq. (13) form a system of eight equations which can be given in matrix form as :

$$\begin{bmatrix} d\bar{t} & d\bar{x} & 0 & 0 & 0 & 0 & 0 & 0 \\ 0 & 0 & d\bar{t} & d\bar{x} & 0 & 0 & 0 & 0 \\ 1 & 0 & 0 & \bar{I} & 0 & 0 & 0 & 0 \\ 0 & 1 & \bar{J} & 0 & 0 & 0 & 0 & 0 \\ 0 & 0 & 0 & 0 & d\bar{t} & d\bar{x} & 0 & 0 \\ 0 & 0 & 0 & 0 & 0 & 0 & d\bar{t} & d\bar{x} \\ 0 & 0 & 0 & 0 & 1/\xi\bar{A} & 0 & 0 & -1 \\ 0 & 0 & 0 & 0 & 0 & 1/\bar{A} & -\lambda & 0 \end{bmatrix} \begin{Bmatrix} \dot{\bar{M}} \\ \bar{M}' \\ \dot{\bar{a}} \\ \bar{a}' \\ \dot{\bar{V}} \\ \bar{V}' \\ \dot{\bar{v}} \\ \bar{v}' \end{Bmatrix} = \begin{Bmatrix} d\bar{M} \\ d\bar{a} \\ 0 \\ \bar{V} \\ d\bar{V} \\ d\bar{v} \\ -\frac{k_1}{k_2}\bar{a} \\ \beta\bar{v} + \eta\alpha f \end{Bmatrix} \tag{14}$$

which can be written as

$$\underset{\sim}{X}\,\underset{\sim}{Z} = \underset{\sim}{W} \tag{14}$$

The Eq. (14) may be used to solve for eight first derivatives of dependent variables if the distribution of the same are known along the initial curve. Solving for $\dot{\bar{M}}$ from Eq. (14) by Crammer's rule yields :

$$\dot{\bar{M}} = \frac{\det Y}{\det X} \tag{15}$$

where det X = determinant of X, and Y is formed by replacing one column of X by $\underset{\sim}{W}$ according to Crammer's rule.

Since the first derivative of the dependent variables may be discontinuous, the derivative M is undetermined. A necessary and sufficient condition for the indeterminancy of $\dot{\bar{M}}$ is det X = 0 and det Y = 0. The vanishing of det X leads to :

$$[\bar{I}(d\bar{t})^2 - \bar{J}(d\bar{x})^2] \cdot [\lambda(d\bar{x})^2/\xi - (d\bar{t})^2] = 0$$

Therefore, either

$$\frac{d\bar{t}}{d\bar{x}} = \pm\sqrt{\bar{J}/\bar{I}} = \pm C_1 \tag{16}$$

or

$$\frac{d\bar{t}}{d\bar{x}} = \pm\sqrt{\lambda/\xi} = \pm C_2 \tag{17}$$

Hence the systems of Eq. (9) are totally hyperbolic since the roots of Eqs. (16 and 17) are real and distinct. The roots $\pm C_1$ (i = 1, 2) are called physical characteristic direction and it is customary to call their inverse as wave velocities.

The vanishing of det Y yields, the compatibility relations along $\pm C_1$ when $\frac{d\bar{t}}{d\bar{x}}$ is replaced by $\pm C_1$ and is given by :

$$\bar{V}\, d\dot{\bar{t}} - \bar{J}\, d\,\dot{\bar{t}} \mp C_1\, d\bar{M} = 0 \tag{18}$$

It can be be very easily verified that solving for $\bar{M}'$, $\dot{\bar{a}}$ and $\bar{a}'$ will lead to an identical set of Eq. (18).

Similarly solving for the remaining derivative, after substitution of $\frac{d\bar{t}}{d\bar{x}} = \pm C_2$ in the appropriate necesssary condition for indeterminancy of derivatives, leads to compatibility relations Eq. (19) along $\pm C_2$:

$$[-\overset{*}{\lambda}\bar{a} \pm \overset{*}{\beta}\bar{v} \pm \overset{*}{\eta}\alpha f]\, d\bar{t} \pm \overset{*}{\lambda}\, d\bar{v} - d\bar{v}/\bar{A} = 0 \tag{19}$$

In the Eq. (19) all asterisked quantities are corresponding unasterisked quantities divided by C_2.

Solution for the dependent variables, in the region where they are continuous, may be obtained by solving Eqs. (18 and 19) simultaneously along the characteristics directions Eqs. (16 and 17) and using initial and boundary conditions Eqs. (11 and 12).

COMPUTATIONAL PROCEDURE

Solution of the system of Eqs. (16 to 19) can be marched out numerically from $\bar{\tau} = 0$ by a step by step integration process. The finite strip in the half plane is divided into a net work as shown in Fig. 3. The dependent variables in this process, are considered as known functions of $\bar{x}$ at a time $\bar{\tau}$, either as given initial conditions or as the output of previous stage computation.

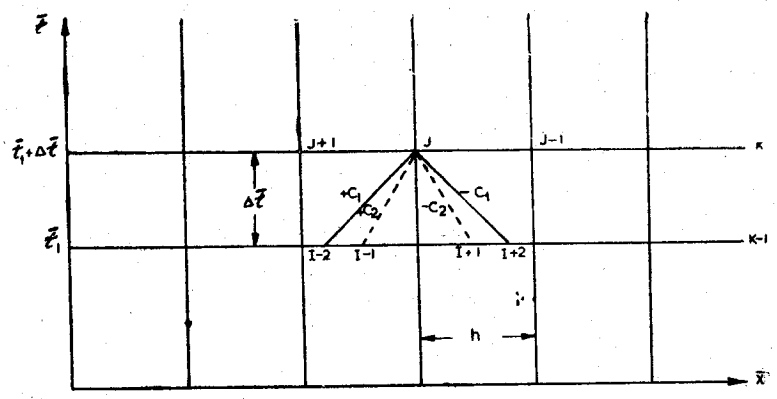

Fig. 3. Interior Grids

Let the dependent variables be known on a line $\bar{\tau} = \bar{\tau}_1$ and are to be evaluated on a line $\bar{\tau} = \bar{\tau}$ on which a typical pivotal point (J.K) is situated as shown in Fig. 3. There are four characteristics $\pm C_1$ and $\pm C_2$ passing through each interior pivotal point. This characteristics intersect the initial line K−1 at four points (I−1,I−2, I+1 and I+2 as shown in Fig. 3) — which hence forth will be called as subgrids. Since coordinate of pivotal point J, K is known, using Eqs. (16 and 17) the space $\bar{x}$ of subgrids may be obtained. Since the cross-section of the monolith is rectangular C_1 and C_2 are constants and Eqs. (16 and 17) in finite difference form reduce to :

$$\bar{x}_{I-2} = \bar{x}_J - \Delta\bar{t}/C_1 \tag{20 a}$$

$$\bar{x}_{I+2} = \bar{x}_J + \Delta\bar{t}/C_1 \tag{20 b}$$

$$\bar{x}_{I-1} = \bar{x}_J - \Delta\bar{t}/C_2 \tag{20 c}$$

$$\bar{x}_{I+1} = \bar{x}_J + \Delta\bar{t}/C_2 \tag{20 d}$$

In the Eq. (20) subscripts refers to the grid or subgrids.

Since the dependent variables are known functions at three adjacent main grid points on the initial line, knowing the coordinates of m th subgrid, a quadratic interpolation formula, as given below, may be used to find each of the variables.

$$\bar{a}_{m\,K-1} = \bar{a}_{J,K-1} - \frac{\bar{x}_J - \bar{x}_m}{2h}(\bar{a}_{J+1,K-1} - \bar{a}_{J-1,K-1}) + \frac{(\bar{x}_J - \bar{x}_m)^2}{2h^2}(\bar{a}_{J+1,K-1} - 2\bar{a}_{J,K-1} + a_{J-1,K-1}) \tag{21}$$

Where $\bar{a}_{J+1,K-1}$ refers to tho function value of $\bar{a}$ at grid point J+1 and on the previous line K−1. $\bar{x}_J$ refers to the space coordinate $\bar{x}$ of point J and a is the grid intervals in $\bar{x}$-direction. Formula similar to the Eq. (21) can be written for the remaining variables.

Now, for a particular pivotal point (J,K) the compatibility relations are written in first order forward difference form in terms of the known values of dependent variables at subgrids. Solving the equation simultaneously for the dependent variables at pivotal point yields the recurrence relation given by

$$\underset{\sim}{U} = B^{-1} D \underset{\sim}{\rho} + B^{-1} \underset{\sim}{Q} \tag{22}$$

where B^{-1}, D = coefficient matrix

$\underset{\sim}{U}$ = dependent variables at pivotal point

$\underset{\sim}{\rho}$ = dependent variables at subgrids

$\underset{\sim}{Q}$ = input ground acceleration

Details of matrices and vectors used in Eq. (22) are given in Appendix–I. In obtaining Eq. (22), it is assumed that $\Delta \bar{t}$ is sufficiently small so that linear relations hold among subgrids and pivotal point and hence averaging of dependent variables may be permitted.

For the vertical boundary plane ($\bar{x} = 0$ and $\bar{x} = 1$), suitable recurrence relation may be obtained using proper boundary conditions and following the procedure similar to the interior mesh points. At left boundary. where $\bar{x} = 0$, two characteristics $-C_1$ and $-C_2$, intersect the boundary pivotal point, J, K (Fig. 4), where boundary conditions from Eq. (12) are :

$$\bar{a}\ (0, \bar{t}) = \bar{v}\ (0, \bar{t}) = 0$$

Knowing the space coordinate of subgrid from Eq. (20b and 20d). the functional value of subgrid m^{th} may be obtained by Taylor series expansion about the pivotal point J+1, K—1, instead of expanding about J, K—1 as is done in Eq. (21), and is given by ,

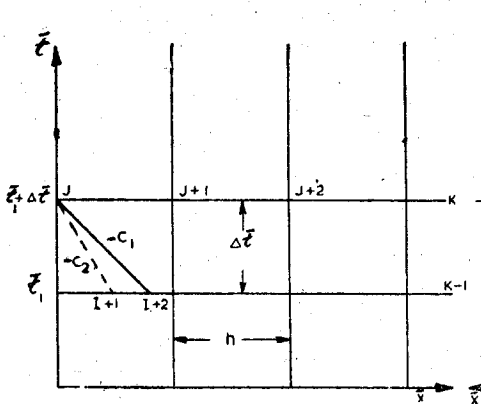

Fig. 4. Left Boundary

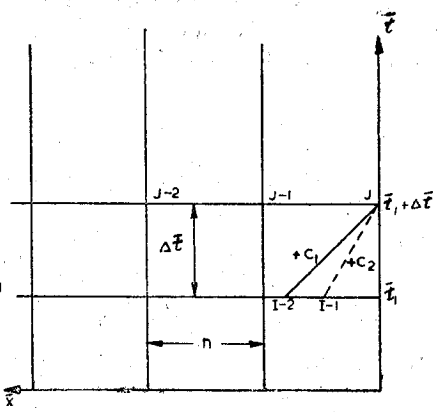

Fig 5. Right Boundary

$$\bar{a}_{m,k-1} = \bar{a}_{j+1,k-1} - \frac{\bar{x}_{j+1} - \bar{x}_m}{2h} (\bar{a}_{j+2,k-1} - \bar{a}_{j,\,k-1}) + \frac{(\bar{x}_{j+1} - \bar{x}_m)^2}{2h^2} (\bar{a}_{j+1,k-1} - 2\,\bar{a}_{j+1,k-1} + a_{j,\,k-1}) \tag{23}$$

Similary introducing known boundary condition in the first order forward difference form of compatibility relations and solving for unknown dependent variables yields :

$$\begin{Bmatrix} \bar{v} \\ \bar{M} \end{Bmatrix}_{j,k} = F^{-1} H \underset{\sim}{L} + \underset{\sim}{F^{-1}} S \tag{24}$$

where F^{-1}, H = coefficient matrix

$\underset{\sim}{L}$ = dependent variables at subgrids

$\underset{\sim}{S}$ = input ground acceleration.

The matrix and vectors used in Eq. (24) are given in Appendix-I.

At the right boundary, $\bar{x} = 1$, two characteristics, $+ C_1$ and $+ C_2$, meet the boundary pivotal point (Fig. 5). Coordinates of subgrids may be obtained using Eqs. (20 a and 20c). The dependent variables of subgrids are evaluated using interpolation formula similar to Eq. (23) by writing a Taylor series expansion about the pivotal point J—1, K—1. Recurrence relation is obtained using identical procedure as left boundary and using proper boundary conditions from Eq. (12) which may be written as :

$$\left\{ \begin{matrix} \bar{a} \\ \bar{v} \end{matrix} \right\}_{j,k} = R^{-1} N \underset{\sim}{T} + R^{-1} \underset{\sim}{M} \qquad (25)$$

where, R^{-1}, N = coefficient matrix

$\underset{\sim}{T}$ = dependent variables at subgrids

$\underset{\sim}{M}$ = ground acceleration

Details of matrix and vectors used in Eq. (25)are given in Appendix-1

Using initial conditions Eq. (11), the solution for the dependent variable ean be marched out with the aid of recurrence relations Eqs. (22, 24 and 25).

NUMERICAL INTEGRATION

The height of the monolith of the dam is divided by main grids at an equal interval ($d\bar{x} = h$). The step size in $\bar{t}$ direction is chosen in accordance with Eq. (16). During integration it is assumed that the accelerogram reading is linear between one peak to subsequent peak. The time interval between subsequent peaks is divided in n equal parts of of step size h (since the cross-section is rectangular, $C_1 = 1$) and remaining $\Delta\bar{t}$ forms another step. Hence, n+1 steps are required for integration from one peak to another. The procedure for integration when $\bar{d}t = d\bar{x} = h$ can be summarised as follows :

Step (1) : The space coordinate of subgrids are located using Eq. (20).

Step (2) : Since $C_1 = 1$ for the problem, the dependent variables at interior subgrids I + 1 and I — 1 in Fig. 3 are interpolated from the known variable at grid point on the initial line, K—1, using a suitable interpolation formula.

Step (3) : Dependent variables at pivotal point are then calculated using proper recurrence relation.

For the remaining part $\Delta\bar{t}$ step (1) and step (3) remain identical except step (2) — where variables at all subgrids have to be interpolated.

By continuously repeating the basic computational steps the solution can be marched out from $\bar{t} = 0$. However, for starting the integration process at $\bar{t} = 0$ initial conditions Eq. (11) have to be utilized.

STABILITY AND CONVERGENCE OF THE NUMERICAL SCHEME

In the case of linear hyperbolic equation the numerical scheme is stable if the sizes for the $\bar{x}$ and $\bar{t}$ variables are chosen to comply with the faster wave velocity[5]. However, convergence of the numerical scheme is tested by changing grid size and accuracy of the same is tested with a problem of which a closed-form solution exists.

The solutions for base shear and base moment of a tapered cantilever Timoshenko beam subjected to a step input of ground acceleration are evaluated for various grid sizes with the help of numerical scheme develeped in this analysis. Peaks of the base shear with time show a little deviation (flater, although the trend is same) at net work of 21 grids from that of 41 and 81 grids. However, the response base moment with time are same of all the grid sizes for all practical purposes (difference in fourth significant figure).

Moreover, the accuracy of this scheme is demonstrated by solving for base shear and base moment of cantilever Timoshenko beam subjected to unit linear velocity, i e. $\bar{v} = 1.$ at base. This beam possesses a material property such that the flexural and shear wave have the same velocity of propagation ($k G = E$). The foregoing problem contains discontinuities along fronts which are taken into account in the programme by tracing out the wave front and by addition of proper jump along it. The numerical results are in good agreement with that obtained by Leonard and Bubianaky (1954) by Laplace transform technique. Error in the numerical analysis is within one percent of closed from solution.

Hence, convergence of the scheme is shown by variation of grid sizes and similarity of results obtained by Leonard and Budianaky (1954) and that obtained by proposed scheme establishes conclusively the stability and aucuracy of the same.

STUDY OF THE KOYNA DAM STRUCTURE

The method developed herein is employed to obtain the transient stresses developed in the highest monolith of the Koyna Dam (Fig. 1) during the earthquake of Dec. 11, 1967. Several combinations of viscous damping ration, μ, and effect of impounded water were considered.

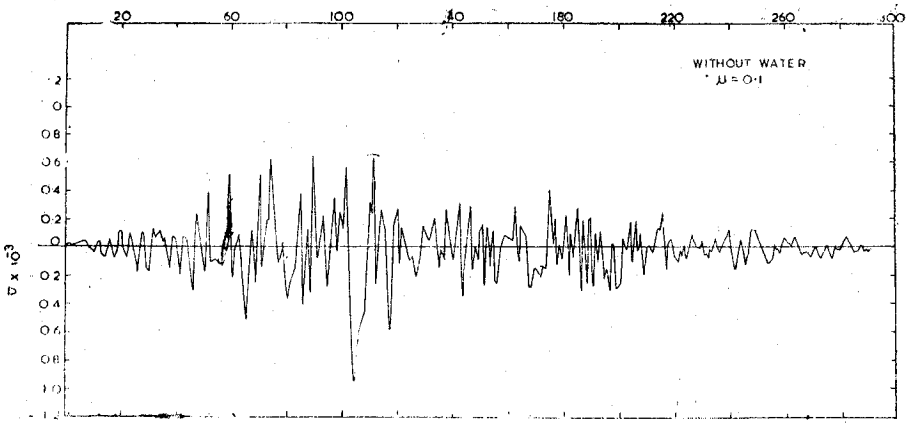

Fig. 6. Shear Force – Time (Section A)

The height of the monolith was divided in thirty four division in such a manner that the node points coincided with the points where the change of slope occurred (points B and C is Fig. 1). Non-dimensional bending stress (σ/E) and shear ($\bar{v}$) were obtained as a function of time for the first ten and three-fourth second of accelerogram record, These quantities are evaluated at base of the monolith, A and at the two points of B and C in Fig. 1. Representative results are shown in Figs. 6 – 9 for the base shear force and bending stress at level C ($\mu = 0.1$ with and without water effect). These results indicate the rapid variation of stresses during the earthquake motion.

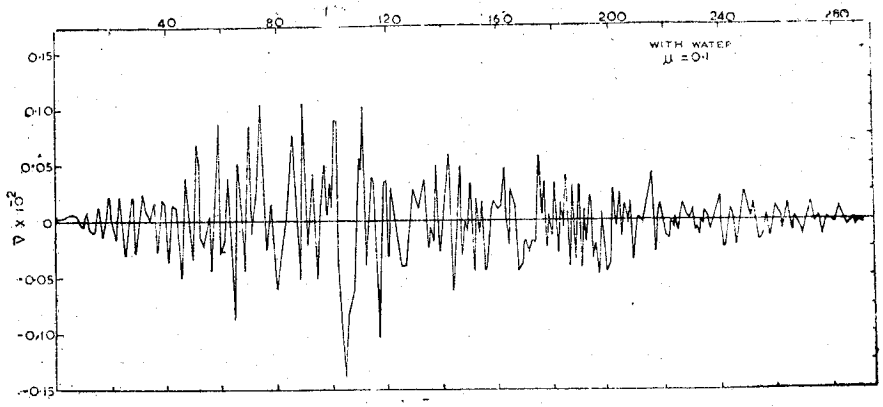

Fig. 7. Shear force-time (Section A)

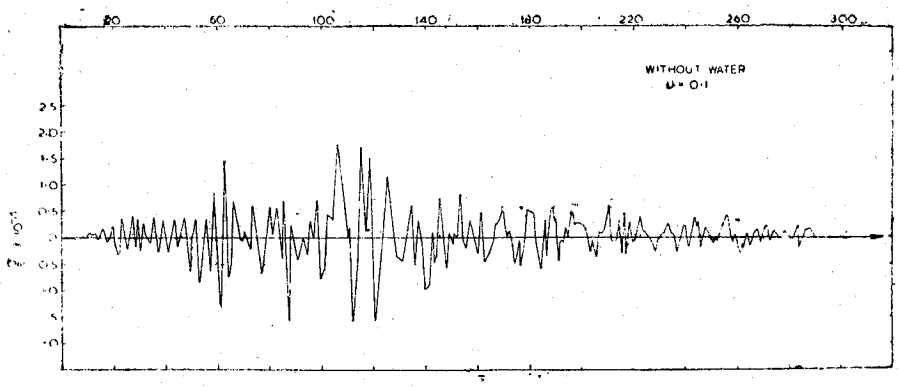

Fig. 8. Bending Stress-time (Section C)

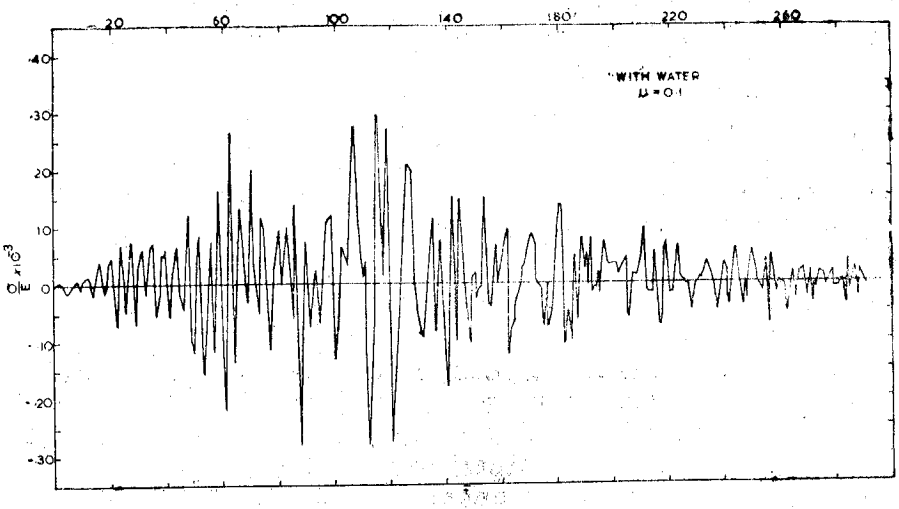

Fig. 9. Bending Stress-time (Section C)

As a part of this study, the bending stress (σ/E) and shear ($\bar{v}$) were obtained by the mode su perposition method. In this approach, the first three modes, frequencies and participation factors were obtained for the monolith, treated as a Timoshenko beam, by numerically integrating the differential equation and searching for the eigen value which satisfied tne determinantal equation.

Next the displacement, velocity and acceleration response spectra were obtained[6]. The maximum response (σ/E) in each of the natural modes were obtained. These values have been tabulated in Table-I.

Table I—Comparison of bending stresses (σ/E)

Section	Mode		Superposition		Proposed Method
	I	II	III	R.M.S.	
	$\tau_1 = 0.34$	$\tau_2 = 0.134$	$\tau_3 = 0.069$		
A	0.0507×10^{-3}	0.183×10^{-4}	$0.323 \times 10\gamma^5$	0.054×10^{-3}	0.17×10^{-3}
B	0.0685×10^{-3}	-0.0669×10^{-4}	-0.0696×10^{-4}	0.0692×10^{-3}	0.175×10^{-3}
C	0.0912×10^{-3}	-0.0505×10^{-3}	0.113×10^{-3}	0.105×10^{-3}	0.294×10^{-3}

From Table I a wide variation is noted between the results of three mode theory and that of the numerical scheme developed in this study. Although the highest peak in the response is quite high compared with three mode theory, the average of the response is quite close to that of mode superposition. Moreover, the maximum step size chosen for step-by-step integration is t = 001121 which is less than one sixth of third mode's time period. Hence the response obtained is more accurate than the three mode theory[1]. The theory of mode superposition always predict average of response rather than maximum value of response and hence the discrepancy with the proposed scheme's results.

The maximum bending stresses are more than the allowable tensile stresses in all three cross-sections of the monolith when hydrodynamic effect of impounding water was considered. The stresses predicted are in higher side owing to the limitation of Zanger's theory. The concept of addition of virtual mass is liable to predict maximum stresses on the higher side than that of actual because the mass of water moving with the dam will not remain constant for the whole interval of time.

However when effect of impounding water is not considered the predicted bending stress is more than allowable value at the cross-section C only.

CONCLUSION

A method to obtain transient response of an elastic structure treated as a continuous problem is presented. This method utilizes the well known method of characteristics and finite difference scheme for step-by-step integration. Stability and convergence of the method is demonstrated by numerical experiments. Furthermore, the solution obtained for the Leonard and Budiansky problem compares very favourably with its known closed-form solution.

The transient response of the highest monolith of Koyna dam for the December 11, 1967 earthquake is obtained. The results indicate that, (a) the response by the persent analysis is much higher than usual mode superposition method, (b) the virtual mass concept accentuates the effect of impounding water, (c) wide variation of stress levels is seen with the change of damping ratio.

For an accurate prediction of the response of the dam structure for a given earthquake the effect of impounding water and the material damping property should be more thoroughly studied.

The method is equally applicable to obtain transient response of other elastic stcructure subjected to dynamic loading.

NOTATIONS

A	Cross-sectional area
A_o	Cross-sectional area at base
$\bar{A}$	Non-dimensional area $= A/A_o$
A_w	Area of water moving with the monolith
$\bar{a}$	Non-dimensional angular velocity $= \frac{L}{k_1}\frac{d\psi}{dt}$
C	Fundamental critical damping $= 2\rho A\omega_1$
$\bar{C}$	Damping constant
C_1, C_2	Families of physical characteristics
C_m	Pressure coefficient
E	Modulus of elasticity
F	$= \eta^* (f_{k-1} + f_k)/4$
f	Non-dimensional forcing function $= \ddot{Z}/g$
G	Shear Modulus
g	Acceleration due to gravity
H	Height of water in Reservoir basin
I	Second moment of area about y-axis
I_o	Second moment of area about y-axis at base
$\bar{I}$	Non-dimensional second moment of area about y-axis $= I/I_o$
J	Rotary intertia about y-axis
J_o	Rotary intertia at base about y-axis
$\bar{J}$	Non dimensional rotary inertia abont y-axis
k	Shape factor
k_1	Velocity of flexural wave $= \sqrt{\frac{E I_a}{P J_o}}$
k_2	Velocity of shear wave $\sqrt{kG/\rho}$
L	Hight of the highest monolith
M	Bending moment

$\bar{M}$	Non-dimensional bending moment $= ML/EI_o$
r	Radius of gyration about y-axis
t	time
$\bar{t}$	Non-dimensional time $= \frac{k_1 t}{L}$
V	Shear force
$\bar{V}$	Non-dimensional shear force $= \frac{VL^2}{EI_o}$
v	Non-dimensional linear velocity $= \frac{1}{k_2}\frac{dw}{dt}$
w	Displacement in Z-direction
$\bar{W}$	Non-dimensional displacement in Z-direction $= w/L$
x	Distance from base
x	Non-dimensional distance from base $= x/L$
$\ddot{Z}$	Ground acceleration
α	$= 1.0 + \frac{\rho_w A_w}{\rho A}$
β	$= \frac{2\mu\,\omega_1\,\rho\,A_o\,L^3\,k_2}{E\,I_o}$
β^*	$= \beta/C_2$
ξ	$= \frac{A_o L^2}{J_o}(k_2/k_1)^3$
λ	$= \frac{k_2 A_o L^2}{k_1 J_o}$
λ^*	$= \lambda/C_2$
μ	= Damping ratio
σ/E	Non-dimensional bending stress
ϕ	Angle of taper with X — axis
ψ	Bending slope
η	$= \frac{\rho g\,A_o\,L^3}{EI_o}$
η^*	$= \eta/C_2$
ω_1	Fundamental frequency
ρ	Mass per unit volume of concrete
ρ_w	Mass per unit volume of water
S	Matrix
$\underset{\sim}{S}$	Row vector
$\underset{\sim}{S}$ or {S}	Column vector
det S or |S|	Determinant
S^t	Transpose of matrix

APPENDIX-1

Details of Matrix, Vector and Determinant

The details of matrices, vectors and determinants used in the analysis of the problem are as follows :

$$B^{-1} = [b^{-1}\,mn/|B|] \quad ; \quad m.\,n = 1, 2, \ldots, 4 \qquad \text{(A 1.1)}$$

where,

$$|B| = -C_1\left(\beta^* d\bar{t}/2 + \lambda^*\right)\left(\frac{JA}{A_{1+1}\,A_{1-1}}\right) + \lambda^* d\bar{t}^2\Big)$$

$$b_{11}^{-1} = b^{-1}{}_{14} = -C_1\,\lambda^* d\bar{t}\,(\beta^* d\bar{t}/2 + \lambda^*)$$

$$b_{12}^{-1} = b_{13}^{-1} = C_1\,J\,(\beta^* d\bar{t}/2 + \lambda^*)/2$$

$$b_{21}^{-1} = b_{24}^{-1} = -C_1\,\lambda^* d\bar{t}\,(A_{1+1} - A_{1-1})/(A_{1+1}\,A_{1-1})$$

$$b_{22}^{-1} = -C_1\,(\lambda^* d\bar{t}^2/2 + J/A_{1+1})$$

$$b_{23}^{-1} = C_1\,(\lambda^* d\bar{t}^2/2 + J/A_{1+1})$$

$$b_{31}^{-1} = b_{34}^{-1} = 2\,A\,C_1\,(\beta^* d\bar{t}/2 + \lambda^*)/(A_{1+1}\,A_{1-1})$$

$$b_{32}^{-1} = b_{33}^{-1} = C_1\,d\bar{t}\,(\beta^* d\bar{t}/2 + \lambda^*)$$

$$b_{41}^{-1} = (\beta^* d\bar{t}/2 + \lambda^*)\left(\frac{A\,J_{1+2}}{A_{1+1}\,A_{1-1}} + \lambda^* d\bar{t}^2/2\right)$$

$$b_{42}^{-1} = b_{43}^{-1} = d\bar{t}\,(\beta^* d\bar{t}/2 + \lambda^*)\,(J_{1+2} - J_{1-2})/4$$

$$b_{44}^{-1} = -(\beta^* d\bar{t}/2 + \lambda^*)\left(\frac{A\,J_{1-2}}{A_{1+1}\,A_{1-1}} + \lambda^* d\bar{t}^2/2\right)$$

$$J_{1+2} = \bar{J}_1 + \bar{J}_{1+2}$$

$$J_{1-2} = \bar{J}_1 + \bar{J}_{1-2}$$

$$J = 2\bar{J}_1 + \bar{J}_{1+2} + \bar{J}_{1-2}$$

$$A = 2\bar{A}_1 + \bar{A}_{1+1} + \bar{A}_{1-1}$$

$$A_{1+1} = \bar{A}_1 + \bar{A}_{1+1}$$

$$A_{1-1} = \bar{A}_1 + \bar{A}_{1-1}$$

$$D = [d_{mn}] \quad , m = 1_2\,2\ldots., 4 : n = 1,2,\ldots,1\,2 \qquad \text{(A 1.2)}$$

where,

$$d_{11} = d_{4\,10} = -d\bar{t}/2$$

$$d_{12} = -C_1$$

$$d_{13} = -J_{-2}/2$$

$$d_{24} = -2/A_{1-1}$$

$$d_{25} = \lambda^* - \beta^* d\bar{t}/2$$

$$d_{26} = d_{39} = \lambda^* d\bar{t}/2$$

$$d_{37} = -2/A_{1+1}$$

$$d_{38} = \beta^* d\bar{t}/2 - \lambda^*$$

$$d_{4\,11} = C_1$$

$$d_{4\,12} = -J_{1+2}/2$$

all other $d_{mn} = 0$; $m = 1, 2, \ldots, 4$; $n = 1, 2, \ldots 12$

$$\underset{\sim}{P} = \{ \bar{V}_{i-2} \quad \bar{M}_{i-2} \quad \bar{a}_{i-2} \quad \bar{V}_{i-1} \quad \bar{v}_{i-1} \quad \bar{a}_{i-1} \quad \bar{V}_{i+1} \quad \bar{v}_{i+1} \quad a_{i+1} \quad \bar{V}_{i+2} \quad \bar{M}_{i+2} \quad \bar{a}_{i+2} \}, \; k-1 \qquad \text{(A1.0)}$$

$$\underset{\sim}{Q}^t = \{0 \quad -F(\alpha_j + \alpha_{i-1})\, d\bar{t} \quad F(\alpha_j + \alpha_{i+1})\, d\bar{t} \quad 0\} \qquad \text{(A 1.4)}$$

$$F = \eta^* (f_{k-1} + f_k)/4$$

In the Eq. (A 1.5) f_k refers to ground acceleration at time $t = K$ and so on

$$F^{-1} = \begin{bmatrix} -A_{i+1}/2 & 0 \\ A_{i+1}\, d\bar{t}/4C_i & 1/C_i \end{bmatrix} \qquad \text{(A 1.6)}$$

$$H = \begin{bmatrix} -2/A_{i+1} & -\lambda^* + \beta^* d\bar{t}/2 & \lambda^* d\bar{t}/2 & 0 & 0 & 0 \\ 0 & 0 & 0 & -d\bar{t}/2 & C_i & -J_{i+2}/I \end{bmatrix} \qquad \text{(A 1.7)}$$

$$\underset{\sim}{L}^T = \{ \bar{V}_{i+1} \quad \bar{v}_{i+1} \quad \bar{a}_{i+1} \quad V_{i+2} \quad \bar{v}_{i+2} \quad \bar{a}_{i+2} \}, k-1 \qquad \text{(A 1.8)}$$

$$\underset{\sim}{S}^T = \{ F(\alpha_j + \alpha_{j-1}) d\bar{t} \quad 0 \} \qquad \text{(A 1.9)}$$

$$R^{-1} = \frac{2}{J_{i-2}(\beta^* d\bar{t}/2 + \lambda^*)} \begin{bmatrix} \lambda^* d\bar{t}/2 & J_{j-2}/2 \\ -(\beta^* d\bar{t}/2 + \lambda^*) & 0 \end{bmatrix} \qquad \text{(A 1.10)}$$

$$N = \begin{bmatrix} -d\bar{t}/2 & -C_i & -J_{j-2}/2 & 0 & 0 & 0 \\ 0 & 0 & 0 & -2/A_{j-1} & \lambda^* - \beta^* d\bar{t}/2 & \lambda^* d\bar{t}/2 \end{bmatrix} \qquad \text{(A 1.11)}$$

$$\underset{\sim}{T}^T = \{\bar{v}_{i-2} \quad \bar{M}_{i-2} \quad \bar{a}_{i-2} \quad \bar{V}_{i-1} \quad \bar{M}_{i-1} \quad \bar{a}_{i-1} \}, k-1 \qquad \text{(A 1.13)}$$

$$\underset{\sim}{M}^T = \{0 \quad -F(\alpha_j + \alpha_{i+1})\, d\bar{t} \} \qquad \text{(A 1.13)}$$

REFERENCES

1. Biggs, J. M., ' Introduction to Structural Dynamics", Mc Graw Hill Inc , New York, 1964.
2. Chopra, A. K., "Earthquake Effects on Dams", Ph. D. Thesis, University of California, Berkeley, 1966.
3. Chou, P. C. and Koeing, H.A., "Journal of Applied Mechanics", Vol. 34, Trans, ASME, Vol. 88, Series E, March 1966, pp. 156-158,
4. Chou, P.C. and Mortimer, R.W., "Journal of Applied Mechanics", Vol. 34, Trans. ASME, Vol. 89 Series E, September 1957, pp. 745-750.
5. Courant, R. and Hilbert, D., "Method of Mathematical Physics", Vol. 2, Interscience Publisher Inc., New York, 1955.
6. Hudson, D. F., Proceeding World Conference on Earthquake Engineering, Berkeley, California, 1956.
7. Jhasman, W. E., Proceeding of 3rd National Congress of Applied Mechanics 1958, pp. 115-202,
8. Leonard, R. W. and Eudiansky, B., NACA Technical Report 1173, 1954.
9. Plass, H.J., Jr., Journal of Applied Mechanics, Vol. 25, Trans. ASME, Vol. 80, September 1958, pp, 379-385
10. Spillers. W. R , Journal of Applied Mechanics, Vol. 32, Trans, ASME, Vol. 87, Series E, June 1965, pp, 346-350.
11. Zanger, C. N., Engineering Monograph No. 11, U. S. Bureau of Reclamation, May, 1962.